Available online at www.sciencedirect.com
SCIENCE DIRECT®
Biochimica et Biophysica Acta 1608 (2004) 35–44
BIOCHIMICA ET BIOPHYSICA ACTA
BBA
www.bba-direct.com

# Energy transfer in monomeric phycoerythrocyanin

Peter Zehetmayer[a], Michaela Kupka[b], Hugo Scheer[b], Andreas Zumbusch[a,*]

[a] Department Chemie, Ludwig-Maximilians Universität München, Butenandtstr. 11, D-81377 Munich, Germany
[b] Department Biologie I- Botanik, Ludwig-Maximilians Universität München, Menzinger Str. 67, D-80638 Munich, Germany

Received 10 June 2003; received in revised form 23 September 2003; accepted 17 October 2003

**Abstract**

Phycoerythrocyanin (PEC) is part of the phycobilisome of cyanobacteria. Its monomer carries one phycoviolobilin and two phycocyanobilins (PCB) as chromophores. For an understanding of the complicated energy transfer in phycobilisomes, a detailed knowledge of the processes in the constituting building proteins is indispensable. We report the experimental data necessary for the description of Förster energy transfer in monomeric PEC, including fluorescence lifetimes and quantum yields of the two subunits. The bulk experiments are complemented by studies of single PEC molecules. Förster energy calculations and Monte Carlo simulations based on the bulk data are presented. They reveal that earlier experimental findings of energy transfer heterogeneities in single PEC molecules originate in spectral shifts between the contributing chromophores.


*Keywords:* Phycoerythrocyanin; Biliprotein; Light harvesting; Energy transfer; Single molecule; Photosynthesis

## 1. Introduction

Antenna complexes of photosynthetic organisms serve as funnels which absorb light and direct excitation energy to the reaction center. Besides increasing the effective absorption cross section of reaction centers and thus allowing efficient light harvesting, an important aspect of their function is to allow the adaptation of the organism to specific light environments. Cyanobacteria contain chromophores belonging to the class of phycobilins, which bridge the green absorption gap of chlorophylls. The phycobilins are open-chain tetrapyrroles which do not contain a metal ion. Unbound to the protein, but also bound to the denatured protein, phycobilin chromophores adopt a 'closed' conformation similar to that of chlorophyll, viz. cyclic tetrapyrroles. Probably due to this symmetric structure, they possess a comparatively low absorption cross section of $\varepsilon \sim 2 \times 10^4$ $M^{-1}$ $cm^{-1}$ in the visible spectral region [1]. In the native biliproteins, to which the chromophores are bound via thioether bonds, they adopt a stretched conformation of the chromophore with a lower symmetry and a significantly increased absorption cross section. There are similarly large differences in excited state dynamics between the chromophores in the native biliproteins and chromophores which are free or bound to the denatured biliproteins. In the latter case, fast internal conversion leads to a relaxation of the electronically excited chromophores within a few picoseconds. By contrast, the lifetime of the excited electronic state is increased to several nanoseconds in the native biliproteins.

In this work we present photophysical studies of phycoerythrocyanin (PEC), a biliprotein which occurs naturally in cyanobacteria as a trimeric or hexameric peripheral constituent of the phycobilisome. Compared to other biliproteins like phycocyanin (PC) or allophycocyanin (APC), relatively little is known about the photophysics of PEC [2–5]. Monomeric PEC consists of two subunits, one of which contains a phycoviolobilin (PVB) chromophore, while the other carries two phycocyanobilins (PCB). PVB and PCB are isomers, but the latter has one carbon double bond more in its conjugated π-system, which leads to a red shift of its excitation and emission spectra with respect to PVB. The X-ray structure of the PEC trimer shows that the interchromophoric distances of the monomer lie in the range between 35 and 48 Å [6]. Therefore, Förster theory [7] is appropriate for the description of the energy transfer between the chromophores.

In spite of at least four different types and a varying number of chromophores, the different cyanobacterial phycobiliproteins are structurally very similar. In particular, PEC is surprisingly similar to PC, with nearly identical distances

* Corresponding author. Tel.: +49-89-2180-77544; fax: +49-89-2180-77545.
*E-mail address:* Andreas.Zumbusch@cup.uni-muenchen.de (A. Zumbusch).

0005-2728/$ - see front matter © 2003 Elsevier B.V. All rights reserved.
doi:10.1016/j.bbabio.2003.10.003

and angles between the chromophores. Based on this similarity and because data for fluorescence spectra, lifetimes, and quantum yields of PEC and its subunits were partly or altogether missing, photophysical data of PC have been used in the analysis of PEC's photodynamics.

For an improved analysis, we now measured the electronic spectra and determined the fluorescence lifetimes and the quantum yields of the α- and β-subunits of the PEC monomer. Based on these data, we calculated the Förster energy transfer rates between the chromophores. As the calculated rates are in the range of the fluorescence lifetimes, we performed Monte Carlo simulations in order to predict the percentage of fluorescence emitted by each of the three chromophores.

The photophysical properties of the biliproteins are very sensitive to the local environment of the chromophores (see above). Because of this high sensitivity to minute structural changes, it is of utmost interest to apply recently developed single molecule detection techniques in studies of photosynthetic pigments. Earlier such studies showed that the emission of individual PEC molecules exhibits pronounced heterogeneities in the energy transfer behavior [8]. An explanation of these heterogeneities requires the knowledge of the energy transfer kinetics in PEC. The occurring energy exchange processes can be modeled with the structural and photophysical parameters which we measured. It is common practice to subsequently derive the averaged molecular properties using Förster theory. In this work, we additionally show how knowledge derived from bulk measurement can be used to explain experimental findings from single molecule measurements. For PEC, variations in the spectra of the three chromophores lead to surprisingly large changes in the energy transfer, which explains the heterogeneities observed in the single molecule experiments. Our results also indicate that dynamic fluctuations of the energy transfer can occur.

## 2. Materials and methods

*Mastigocladus laminosus* (*Fischerella* PCC7603) was cultivated in Castenholz-Medium [9] at 50 °C under green light. After harvesting, cells were stored at −20 °C. PEC was isolated by adaptation of the methods of Füglistaller et al. [10], Parbel [11] and Reuter [12]. Briefly, *M laminosus* cells (28 g) were suspended in 50 mM $KH_2PO_4/K_2HPO_4$ buffer at pH 7, broken by ultrasound (pulsed mode with a duty cycle of 50% and 130 W) and centrifuged at 36 000 × *g* for 30 min. The supernatant was fractionated by precipitation with $(NH_4)_2SO_4$ (first 30% and then 70%). The pellet from 70% precipitation was resuspended in 5 mM $KH_2PO_4/K_2HPO_4$ buffer and dialysed against 5 mM $KH_2PO_4/K_2HPO_4$ buffer overnight. The dialysate was loaded onto a DEAE-Cellulose column (140 ml) and fractions were collected according to UV–Vis absorption properties. The isolated PEC was further purified by preparative, native PAGE (6%) [13]. Three bands were eluted from the gel, PEC-Trimer, PEC with the large linker and PEC with the small linker protein. PEC monomer was obtained by adding urea (final concentration 4 M) to the trimeric PEC solution. α- and β-subunits were isolated by isoelectric focusing as has been described elsewhere [14].

Steady-state absorption spectra were recorded with a Perkin Elmer 330 (Perkin Elmer, Germany) spectrometer. Fluorescence excitation and emission spectra were acquired using an Edinburgh Instruments FS900 spectrometer (Livingston, UK). For the determination of fluorescence lifetimes, a time-correlated single photon counting (TCSPC) setup was used. It consisted of a laser system with a 10-W Nd:$YVO_4$ pump laser (Millenia X, Spectra-Physics, Mountain View, USA), a Ti-Sapphire oscillator (Tsunami, Spectra-Physics, Mountain View, USA), an optical parametric oscillator with a frequency doubler (OPAL, Spectra-Physics, Mountain View, USA), and provided 100-fs excitation pulses tunable over the entire visible spectral region. The fluorescence signal was collected in a 90° geometry and passed through a monochromator (H10D, Jobin-Yvon, Longjumeau, France). It was detected with a multi-channel plate (C2773-02, Hamamatsu, Hamamatsu City, Japan) connected to fast counting electronics (SPC 300, Becker&Hickl, Berlin, Germany). The observed instrument response function had a width of 70 ps. Average lifetimes were calculated as follows [15]:

$$\langle t\rangle = \frac{\int tI(t)\mathrm{d}t}{\int I(t)\mathrm{d}t}$$

The single molecule setup has been described in detail elsewhere [8]. Briefly, excitation light from an $Ar^+$-Laser (Innova 90-6, Coherent Inc., St. Clara, USA) was focused onto the sample with a high numerical aperture objective (Nikon Plan Apochromat 60 ×, NA 1.2, water immersion). A back-reflection geometry was used to collect the fluorescence light. The signal was filtered with a dichroic mirror (575 DCXR, Chroma, Brattleboro, USA) and suitable holographic filters (HNPF-568-10, Kaiser Optical Systems, Inc., Ecully, France) before detection with a single-photon counting module (SPCM-AQR-16, EG&G Inc., Gaithersburg, USA). For simultaneous detection of two polarization components, a polarizing beamsplitter was brought into the detection path. In this case two single photon counting modules were used for the detection. Images were created by raster scanning the sample with a piezo positioning unit (P-731, Physik Instrumente, Karlsruhe, Germany).

For the calculation of Förster energy transfer rates, we assumed an orientation of the transition dipole moments along the long axis of the chromophores (see Fig. 1). In the case of the α-84 PVB, only the conjugated ring system was considered. The distances of the chromophores were derived from the X-ray structure [6]. A refractive index of $n = 1.34$, which Moog et al. [16] have shown to be appropriate for the globin protein environment, was used in the calculations.

Monte Carlo simulations were performed in order to account for the competition between energy transfer and

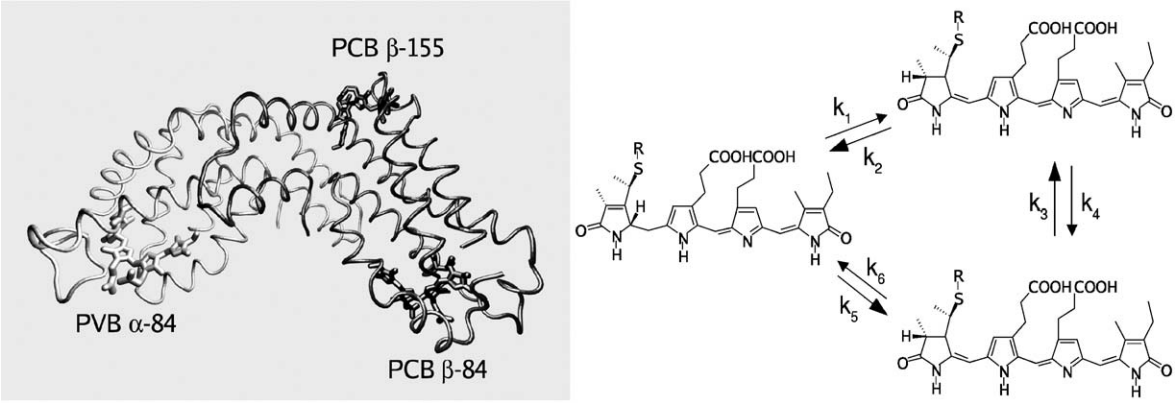


Fig. 1. Structure of monomeric PEC derived from the trimer X-ray structure [6]. The distances between the chromophores are, $R$(α-84/β-84) = 48 Å, $R$(α-84/β-155) = 47 Å, and $R$(β-84/β-155)=35 Å. The energy transfer rates between the chromophores are calculated on basis of the experimental data described in the text to be $k_1 = 1.44\ ns^{-1}$, $k_2 = 0.13\ ns^{-1}$, $k_3 = 2.56\ ns^{-1}$, $k_4 = 14.20\ ns^{-1}$, $k_5 = 10.45\ ns^{-1}$, and $k_6 = 0.28\ ns^{-1}$.

relaxation of the individual chromophores. The system contains three chromophores, A, B, and C. The probabilities for energy transfer from chromophore A to the respective neighboring chromophores are given by the rates $k_{AB}$ and $k_{AC}$. By contrast, the direct relaxations rates of chromophore A, comprising internal conversion, intersystem crossing, photochemical processes and fluorescence, are grouped in the rate $k_A$. Assuming that the excitation is located on chromophore A, the probability that a process occurs, which is described by the rates $k_{AB}$, $k_{AC}$ or $k_A$, must sum up to 1. For the simulation three intervals are defined, which represent the two possible energy transfer pathways or the relaxation. The size of the intervals is equivalent to the probability with which either one of the two energy transfer pathways or relaxation of the chromophore occurs. The probability interval size thus corresponds to the respective normalized probability $k/k_{tot}$ with $k_{tot} = k_{AB} + k_{AC} + k_A$. Similar probability intervals are calculated for energy transfer starting from one of the other chromophores. The simulation starts with an excitation localized on one chromophore. Pseudo-random numbers in the interval [0,1] are subsequently obtained from a modified Mersenne Twister generator [17]. The path of the excitation is determined by the interval to which the random number belongs. If, after the simulation step, the excitation is still on one of the chromophores, subsequent simulation steps with the appropriate rates are performed until the excitation is removed from the system by relaxation. Altogether $10^7$ simulations were made for each of the three different initial excitation locations.

## 3. Results and discussion

Förster energy transfer between a donor D and an acceptor A is given by:

$$k_{DA} = \frac{9000 \ln 10 \phi \kappa^2}{128 \pi^5 n^4 N_A \tau_D R^6} \int f(\tilde{\nu}) \varepsilon(\tilde{\nu}) \frac{d\tilde{\nu}}{\tilde{\nu}^4} \quad (1)$$

The required photophysical and geometrical parameters therefore are: the fluorescence quantum yield $\phi$, the fluorescence lifetime $\tau_D$, the absorption spectrum $\varepsilon(\tilde{\nu})$ of the acceptor, the fluorescence spectrum $f(\tilde{\nu})$ of the donor, the respective chromophore orientation described by $\kappa$, the distance $R$ between donor and acceptor and the refractive index $n$.

### 3.1. Fluorescence excitation and emission spectra

A detailed knowledge of the steady state absorption and fluorescence emission spectra of the individual chromophores present in PEC is basis to any understanding of its energy transfer behavior. In PEC as well as in PC, the problem is to disentangle the spectra of the multichromophoric monomers and to correctly assign the observed spectral components to the respective chromophores. As PEC and PC each contain only one chromophore in the α-subunit, it is straightforward to measure the absorption and fluorescence spectra of the isolated α-subunit [14,18]. The measured absorption and fluorescence emission spectra for the α-subunit of PEC are well represented by a sum of two Gaussian functions (Fig. 2). A similar procedure, including four Gaussian functions, has previously been used for the modeling of PEC spectra [14]. Our simpler model, however, appropriately describes the spectra and is better suited for the calculation of spectral overlap integrals which are needed for the determination of Förster energy transfer rates.

The α-subunit absorption spectrum shows an additional short wavelength component. This is due to the well-known light-driven Z/E-isomerization of PVB, which leads to the formation of the E-form with an absorption maximum at 507 nm [19]. It is therefore not possible to match the high energy part of the absorption spectrum of the Z-form with the fitting function. However, care was taken to properly model the lower energy part of the absorption spectrum of the α-84 PVB, which is the crucial part for the calculation of the overlap integrals with the emission of the β-subunit chro-

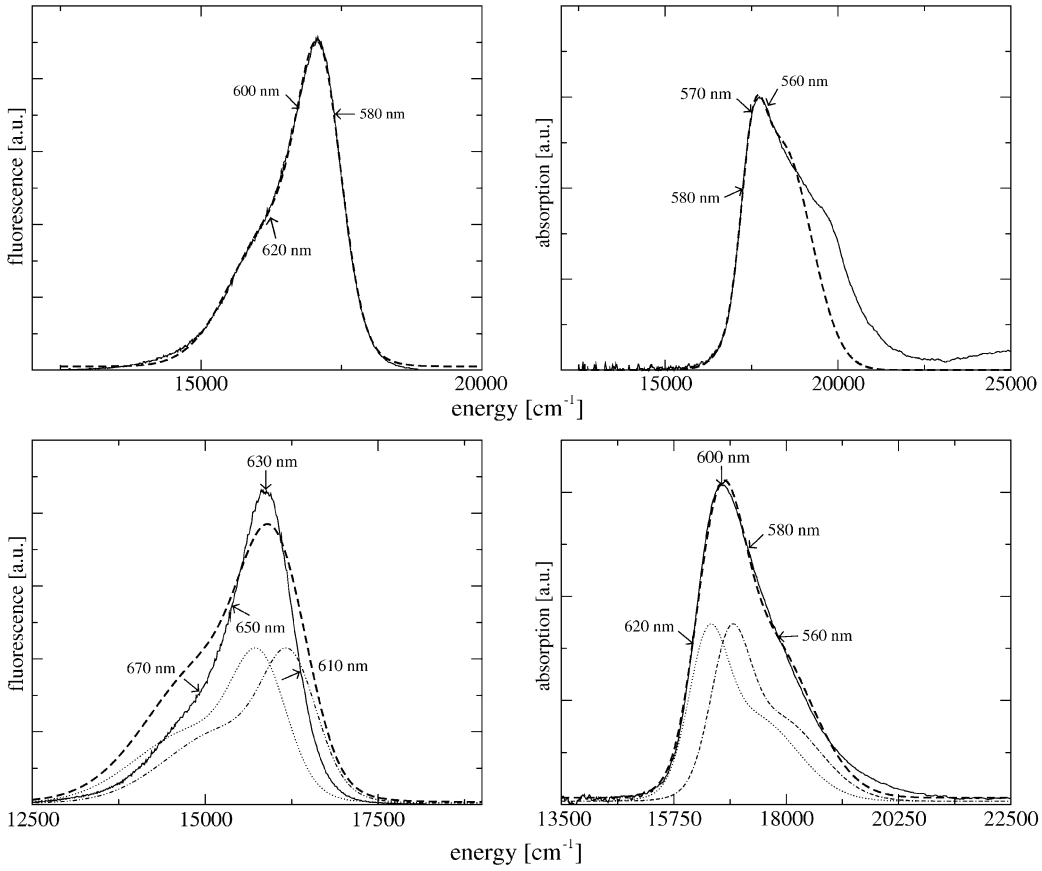


Fig. 2. Absorption and fluorescence spectra (solid line —) of the α-(top) and β-subunit (bottom). The respective fits are depicted as dashed lines (– – – –). For the β-subunits, the spectra derived for the individual PCB chromophores are also shown (β-84: -·-·-, β-155: ·····). The arrows indicate the experimentally used excitation and detection wavelengths on the wavelength scale, respectively.

mophores. Over the whole spectral range, the fluorescence emission spectrum of the α-subunit is well represented by the fitting function. Note that for the emission spectrum no complication arises from the presence of two PVB isomers, as the E-form has been shown to be only very weakly fluorescing [20].

Problems arise in the analysis of the β-subunit, which carries two PCB chromophores. The previously controversial [2,4] assignment of the optical spectra to the chromophores has been achieved recently, based on steady-state absorption and circular dichroism spectroscopy [14]. For each PCB chromophore, we also used a sum of two Gaussian functions in order to describe the spectra. Assuming that both chromophores contribute equally to the absorption, we used identical amplitudes, $a_1$ and $a_2$, in the sum of the two fitting functions. In addition, the widths $b_1$ and $b_2$ and $\delta s = x_1 - x_2$ were kept the same for both chromophores:

$$A(\tilde{\nu}) = a_1 e^{\frac{-(\tilde{\nu}-x_1)^2}{b_1^2}} + a_2 e^{\frac{-(\tilde{\nu}-x_2)^2}{b_2^2}} + a_1 e^{\frac{-(\tilde{\nu}-x_3)^2}{b_1^2}} + a_2 e^{\frac{-(\tilde{\nu}-x_3-\delta s)^2}{b_2^2}}$$

The absorption spectrum of the β-subunit is well described with this function and the contributions from the β-84 and the β-155 chromophores are identified. The fluorescence emission spectrum of the β-subunit can be considered to be dominated by the emission of the energetically lower-lying β-84 chromophore. Therefore, the comparison of the β-84 calculated absorption spectrum and the experimentally determined emission spectrum of the β-subunit yields the Stokes shift for β-84. The Stokes shift of the β-155 PCB is assumed to be the same. Both emission spectra are finally obtained by using the mirror image of their absorption spectra and shifting them by the determined Stokes shift. This procedure is justified as the absorption and the emission spectra of the β-subunit, which contains two PCB chromophores, are mirror images. The absorption and emission maxima for all chromophores are: $\lambda_{abs}$(α-84) = 564 nm, $\lambda_{em}$(α-84) = 586 nm, $\lambda_{abs}$(β-84) = 606 nm, $\lambda_{em}$(β-84) = 636 nm, $\lambda_{abs}$(β-155) = 590 nm, $\lambda_{em}$(β-155) = 619 nm. The fitting parameters are collected in Table 1. Our data are in very good agreement with those of Parbel et al. [14] with the advantage of being modeled in a simpler form.

### 3.2. Fluorescence quantum yields

No data have been published to date for the fluorescence quantum yields of PEC and its individual chromophores. We determined the quantum yields for all chromophores by comparison to reference dyes with known quantum yields

Table 1
Fitting parameters for the description of the individual chromophore spectra

| | $a_1$ | $x_1$ [cm$^{-1}$] | $b_1$ [cm$^{-1}$] | $a_2$ | $x_2$ [cm$^{-1}$] | $b_2$ [cm$^{-1}$] |
|---|---|---|---|---|---|---|
| *Absorption* | | | | | | |
| α-84 | 50729 | 17539 | 486 | 89335 | 18376 | 1185 |
| β-84 | 71896 | 16430 | 536 | 47499 | 17346 | 1217 |
| β-155 | 71896 | 16873 | 536 | 47499 | 17788 | 1217 |
| *Emission* | | | | | | |
| α-84 | $2.88\times10^{-4}$ | 16345 | 1107 | $4.62\times10^{-4}$ | 17125 | 532 |
| β-84 | $4.21\times10^{-4}$ | 15792 | 536 | $2.78\times10^{-4}$ | 14877 | 1217 |
| β-155 | $4.21\times10^{-4}$ | 16234 | 536 | $2.78\times10^{-4}$ | 15391 | 1217 |

For β-155, $x_1$ corresponds to $x_3$, while for $\delta s = x_2 - x_1$, a constant value of −916 cm$^{-1}$ was used. Absorption bands are normalized to the extinction coefficient in the maximum, emission bands are normalized to unity.

$\phi_r$ and spectra similar to the PEC chromophores using the following expression [21]:

$$\phi_u = \frac{A_r F_u n_u^2}{A_u F_r n_r^2}\phi_r$$

Here $A$ is the absorption at the reference wavelength, $F$ is the integrated fluorescence spectrum and $n$ is the refractive index. The indices u and r designate the unknown dye, in our case the biliprotein, and the reference dye, respectively. Rhodamine 101 ($\phi_r = 100\%$) was used as a reference dye for the α-84 PVB and $\phi_{\alpha\text{-}84}$ was determined as a function of the excitation wavelength. Hardly any variation of $\phi_{\alpha\text{-}84}$ was observed in the spectral range from 545 to 572 nm. In this region, the spectra of the reference dye and the α-subunit coincide well, while they diverge at higher energies due to the contribution of the E-isomer of PVB. Therefore, no reliable determination of $\phi_{\alpha\text{-}84}$ is possible at $\lambda < 545$ nm. The maximum value of $\phi_{\alpha\text{-}84}$ is 0.19 at 557 nm, while the calculated mean is 0.17. These data compare well to $\phi = 0.23$ determined for the α-84 PCB chromophore in PC [22].

The absorption spectrum of cresyl violet superimposes perfectly with that of the β-subunit. Cresyl violet was thus chosen as a reference dye ($\phi_r = 54\%$). A mean quantum yield of $\phi_\beta = 0.27$ was determined between 521 and 615 nm, with a pronounced maximum of 0.37 at 598 nm. While the origin of this peak in $\phi_\beta$ is not clear, it should be noted that only the mean value of $\phi_\beta$ over the absorption band is of importance for the calculation of the energy transfer rates. Previously, the quantum yields of the two PCB chromophores in the β-subunit of PC have been estimated to be $\phi_{\beta\text{-}84} = 0.19$ and $\phi_{\beta\text{-}155} = 0.25$. This estimation was based on a comparison of the fluorescence lifetimes between the β-subunit chromophores and of α-84 PCB in PC [22]. From our experiments, we are not able to distinguish the contributions from the two chromophores in the β-subunit. Based on the results from the mutation experiments on PC [22], one can however conclude that no large differences in the quantum yields of the two chromophores exist. We therefore assume the measured mean value of $\phi_\beta = 0.27$ for each β-subunit chromophore in PEC in the energy transfer calculations, which is somewhat higher than that of β-PC.

### 3.3. Fluorescence lifetimes

Since the excitation and emission spectra, the quantum yields, and the geometry of PEC are now known, the fluorescence lifetimes of each chromophore are the only remaining unknown parameters for the calculation of the energy transfer in monomeric PEC. As this information was previously lacking, it has been common practice to use estimated values in the description of energy transfer in biliproteins. Only recently have lifetimes for specific chromophores of biliproteins been determined. For the PCB in PC, it was found that the α-84 has a lifetime of 1.50 ns, which is close to the value of 1.45 ns determined for the β-84 chromophore. The authors were also able to give a value of 0.93 ns for the β-155 PCB, even if this value has a larger error margin [22]. It was unfortunately not reported whether also additional faster components were observed. For PEC, lifetimes of a dissociation product PEC(X), which is believed to be similar to the α-subunit of PEC, and of monomeric PEC were reported previously [2]. The preparation of monomeric PEC, however, afforded treatment with KSCN which leads to spectral changes.

In order to minimize influences from the preparation of the monomers, the more benign preparation with 4 M urea, which does not lead to observable spectral changes [14], was chosen in this work. The fluorescence lifetimes of the α-subunit and the β-subunit of PEC were measured for the first time. Different excitation and detection wavelengths were used. In spite of the α-subunit containing only a single PVB chromophore, we nevertheless found triexponential decay kinetics in all cases, with two major components at around 200 and 600 ps, and also a minor slower component (cf. Table 2). While the lifetimes of the two shorter lived components do not change when the detection wavelength

Table 2
Fluorescence decay times τ, amplitudes $A$, and their averages $\langle t \rangle$ of the α-subunit observed for different excitation and emission wavelengths

| Emission wavelength | Excitation wavelength | | | | | |
|---|---|---|---|---|---|---|
| | 560 nm | | 570 nm | | 580 nm | |
| | $A$ | τ [ps] | $A$ | τ [ps] | $A$ | τ [ps] |
| 580 nm | 0.41 | 332 | 0.33 | 230 | | |
| | 0.42 | 627 | 0.50 | 615 | | |
| | 0.17 | 1174 | 0.18 | 1283 | | |
| $\langle t \rangle$ | | 738 | | 817 | | |
| 600 nm | 0.39 | 269 | 0.39 | 301 | 0.14 | 117 |
| | 0.43 | 573 | 0.44 | 616 | 0.74 | 635 |
| | 0.17 | 1243 | 0.17 | 1391 | 0.11 | 1885 |
| $\langle t \rangle$ | | 768 | | 848 | | 1013 |
| 620 nm | 0.17 | 100 | 0.39 | 230 | 0.21 | 156 |
| | 0.61 | 426 | 0.48 | 613 | 0.68 | 633 |
| | 0.22 | 1153 | 0.13 | 1456 | 0.11 | 1840 |
| $\langle t \rangle$ | | 767 | | 839 | | 982 |

is varied, there is a clear increase of the longest living component's lifetime with increasing excitation wavelength. The averaged lifetimes thus varied between 738 and 1013 ps. The origin of the complicated decay pattern of the α-subunit is not clear. One complication arises from the Z/E-isomerization of PVB, which leads to the existence of two different PVB populations. However, also the isolated α-subunits of PC and APC, which contain a single chromophore that does not isomerize, are multiexponential. It has already been pointed out previously that conformational heterogeneities of biliproteins may exist [3]. Further evidence for this hypothesis comes from recent single molecule experiments [8]. Whether such heterogeneities occur naturally or whether they are induced by the separation and isolation of the subunits cannot be judged from the available experimental data.

In contrast to the α-subunit, we observe the expected simple decay behavior for the β-subunit, which carries two PCB chromophores. Here, consistently two decay components are found which show no dependence on the excitation and detection wavelength. In all cases we find approximately equally important components with a lifetime of 308 to 572 ps (40%) and 1291 to 1473 ps (60%). The mean lifetimes were determined to be 1163 to 1296 ps.

Based on the complicated decay kinetics of the isolated α-subunit, and assuming that it is not an artifact of the isolation, a correspondingly complicated pattern is expected for experiments with PEC monomers composed of the α- and the β-subunit. This is verified by the kinetic data in Table 3. With the exception of the experiments with excitation at 620 nm, all decay curves had to be fitted with three exponential components, which were furthermore emission wavelength-dependent. In the case of long-wavelength excitation (620 nm), we find exactly the same behavior as for the isolated β-subunits with a biexponential decay comprising a slow and a fast component with time constants of 1400 and 315 ps, respectively. This may have been anticipated, because the α-subunit hardly has any absorption at this wavelength and uphill transfer to the PVB-chromophore ($\lambda_{max}$ = 564 nm) is unlikely. It is, however, an important finding which indicates that the aggregation of the two subunits does not change the emission kinetics of the β-subunit. The data are less readily interpreted for shorter excitation wavelengths, where both the α- and the β-subunit exhibit significant absorption. One clear trend is the decrease of the slowest decay lifetime with increasing excitation wavelength. This can be explained by Förster energy transfer. Direct excitation of the α-chromophore leads to fast and nearly irreversible resonance energy transfer to the β-subunit. As a consequence, the α-subunit fluorescence becomes quenched, while the observed lifetime of the β-subunit becomes longer [23]. At an excitation wavelength of 600 nm, an intermediate behavior is observed, in which most of the fluorescence emission originates from direct β-subunit excitation and only a minor part is due to previous energy transfer from the α-subunit. This complicated mix of several contributions is even more pronounced for the short decay components. It has been detailed above that the isolated α-subunit exhibited two, while the β-subunit showed one fast component. Energy transfer between the subunits will then lead to the emergence of additional fast components. Triexponential fitting functions represent the experimental data well within the given signal/noise ratio, even if we expect much more complicated decay dynamics on the sub-nanosecond time scale. These, however, cannot be resolved into several clearly separated components. A detailed analysis of the energy transfer therefore has to be based upon energy transfer calculations using the experimentally accessible photophysical data from the subunits and the X-ray structure of PEC.

Table 3
Fluorescence decay times τ, amplitudes *A*, and their averages ⟨*t*⟩ for different excitation and emission wavelengths in monomeric PEC

| Emission wavelength | Excitation wavelength | | | | | | | |
|---|---|---|---|---|---|---|---|---|
| | 560 nm | | 580 nm | | 600 nm | | 620 nm | |
| | *A* | τ [ps] | *A* | τ [ps] | *A* | τ [ps] | *A* | τ [ps] |
| 610 nm | 0.36 | 179 | 0.22 | 101 | 0.17 | 119 | | |
| | 0.40 | 704 | 0.42 | 526 | 0.45 | 490 | | |
| | 0.24 | 1782 | 0.45 | 1737 | 0.38 | 1528 | | |
| ⟨*t*⟩ | | 1264 | | 1379 | | 1218 | | |
| 630 nm | 0.14 | 111 | 0.28 | 266 | 0.10 | 127 | 0.53 | 316 |
| | 0.48 | 574 | 0.43 | 900 | 0.46 | 513 | 0.47 | 1395 |
| | 0.38 | 1724 | 0.29 | 2067 | 0.44 | 1581 | | |
| ⟨*t*⟩ | | 1361 | | 1514 | | 1290 | | 1172 |
| 650 nm | 0.28 | 257 | 0.26 | 259 | 0.08 | 107 | 0.53 | 313 |
| | 0.44 | 860 | 0.42 | 821 | 0.48 | 510 | 0.46 | 1388 |
| | 0.27 | 1941 | 0.33 | 1962 | 0.44 | 1588 | | |
| ⟨*t*⟩ | | 1401 | | 1484 | | 1297 | | 1164 |
| 670 nm | 0.31 | 266 | 0.35 | 308 | 0.32 | 295 | 0.54 | 318 |
| | 0.48 | 901 | 0.41 | 989 | 0.44 | 891 | 0.46 | 1463 |
| | 0.21 | 2056 | 0.23 | 2049 | 0.24 | 1895 | | |
| ⟨*t*⟩ | | 1374 | | 1419 | | 1316 | | 1142 |

### 3.4. Geometric parameters

The center-to-center distances between the chromophores in monomeric PEC are 35 Å for β-84/β-155, 48 Å for α-84/β-84, and 47 Å for α-84/β-155. Therefore, Förster resonance energy transfer is expected to be the only relevant energy transfer process between the chromophores [7]. The respective orientational parameters are $\kappa^2$(β-84/β-155) = 0.68, $\kappa^2$(α-84/β-84) = 2.82, and $\kappa^2$(α-84/β-155) = 0.36 (see Materials and methods).

### 3.5. Calculations of the energy transfer in monomeric PEC

Based on the set of photophysical parameters collected in Table 4, the refractive index *n* = 1.34, and the geometric data listed above, the Förster resonance energy transfer rates can be calculated. The results of these calculations are collected in Fig. 1.

α-84 is responsible for absorption of high energy light (530–580 nm) in PEC. The transition dipole is oriented very

Table 4
Photophysical parameters used in the Förster calculations, with the overlap integral $J(\tilde{\nu})$ being defined as $J(\tilde{\nu}) = \int f(\tilde{\nu})\varepsilon(\tilde{\nu})((d\nu)/\nu^4)$, the fluorescence lifetime $\tau_D$, and the fluorescence quantum yield $\phi$

| Acceptor | Donor | | | | |
|---|---|---|---|---|---|
| | α-84 | β-84 | β-155 | $\tau_D$ | $\phi$ |
| | $J(\tilde{\nu})$ [$M^{-1}$ $cm^3$] | $J(\tilde{\nu})$ [$M^{-1}$ $cm^3$] | $J(\tilde{\nu})$ [$M^{-1}$ $cm^3$] | [ps] | [%] |
| α-84 | – | $1.87 \times 10^{-14}$ | $6.06 \times 10^{-14}$ | 800 | 17 |
| β-84 | $7.52 \times 10^{-13}$ | – | $5.84 \times 10^{-13}$ | 1200 | 27 |
| β-155 | $7.05 \times 10^{-13}$ | $1.05 \times 10^{-13}$ | – | 1200 | 27 |

favorably for fast energy transfer towards β-84. Just the opposite is true for its orientation with respect to β-155. For this reason and in spite of very similar spectra and distances between the respective chromophores, energy transfer is much faster between α-84 and β-84 than between α-84 and β-155. In both cases, however, the ratios between the backward and forward transfer rate constants (3% and 9%, respectively) indicate that energy absorbed by α-84 is nearly irreversibly transferred to the β-subunit chromophores. For the two PCB chromophores in the β-subunit, the orientation is not optimal for fast energy transfer between them. Here however, the relatively close distance of 35 Å, corresponding to 0.63 times the Förster radius, nevertheless leads to fast energy distribution. Although the ratio of the backward and forward rate constants is increased to 18% in this case, most of the excitation will eventually end up at the β-84 chromophore.

It is interesting to compare the energy transfer in the monomers of PEC and in PC. They have very similar structures [6,24] and basically differ by the replacement of a low energy ($\lambda_{max} = 624$ nm) [18] PCB with a high energy ($\lambda_{max} = 564$ nm) PVB chromophore. The distances between the chromophores in monomeric PC are 34 Å for β-84/β-155, 48 Å for α-84/β-84, and 51 Å for α-84/β-155. One obtains $\kappa^2$ (β-84/β-155) = 0.59, $\kappa^2$ (α-84/β-84) = 2.96, and $\kappa^2$ (α-84/β-155) = 0.18. The electronic spectra of the two pigments are however quite different. The spectra of all chromophores in PEC are blue shifted by approximately 30 nm compared to PC and their energetic ordering is changed. In PEC from *M. laminosus*, the energetic ordering is α-84>β-155>β-84. It is changed to β-155>α-84>β-84 in PC from *Synechococcus* sp. PCC 7002 [22]. We note that the calculated energy transfer rate ratios show that energy from light absorbed by the highest energy absorber (α-84 in PEC and β-155 in PC) is transferred much more efficiently to the energetically lowest-lying β-84 chromophore in PEC than in PC, where the respective rate ratios are 15% (β-155/α-84), 10% (β-155/β-84), and 65% (α-84/β-84). The reason for this is that only the energetic ordering but not the orientation of the chromophores is different in PC with respect to PEC. In both cases, the orientational parameter $\kappa^2$ is optimal for fast energy transfer between α-84 and β-84. The spectral overlap integrals are also similar for PC and PEC.

The energy transfer in both PEC and PC takes place on time scales similar to that of the fluorescence decay. In order to assess the question from which chromophore fluorescence or non-radiative relaxation occurs, we chose to perform Monte Carlo simulations for a complete modeling. The results of these simulations are summarized in Table 5. In the Förster picture, an excited donor molecule transfers its energy to an acceptor molecule with a given energy transfer rate. Fluorescence from the donor is a process competing with the energy redistribution via the Förster mechanism. Therefore, excitation of one chromophore in monomeric PEC leads to a distribution of excitation energy among all three chromophores. This can be described by a differential equation system. If the competitive fluorescence process is neglected, this results in the so-called stationary solution (cf. Table 5). If, however, fluorescence emission is taken into account, the distribution of excitation energy can be probed by measuring the fluorescence originating from the individual chromophores. While in a bulk sample this is experimentally not feasible and because the differential equation system is not solvable with the available experimental data, a Monte Carlo simulation is performed in the following manner: After locating the excitation on one specific chromophore, the energy transfer rates and the fluorescence decay rate are describing the probability for the systems development. By counting the relaxation events via fluorescence, the fluorescence intensities for the individual chromophores in PEC can be simulated. The deviations between the simulation results and the stationary solution of the differential equation system clearly show that fluorescence relaxation channels must be taken into account.

In the simulation, we observe that different results are obtained depending on which chromophore the initial excitation was localized. If one of the PCB chromophores is the initial absorber, the results are essentially indistinguishable from the static Förster calculations. If, however, the α-84 PVB acts as the initial absorber, its fast relaxation, either radiationless or via fluorescence, has an important influence on the decay pattern of the PEC monomer. Under these circumstances, 12% of the excitation energy relaxes via the α-84 chromophore. This behavior will, however, change drastically if PEC forms trimeric or hexameric complexes. In these naturally occurring aggregates, the α-84 and the β-84 chromophores of different monomers have a distance of only 20 Å [6]. This will give rise to an additional very

Table 5
Distribution of the energetic relaxation from the different chromophores

| Emission | Location of initial excitation | | | |
|---|---|---|---|---|
| | α-84 | β-84 | β-155 | Stationary solution |
| α-84 | 12 | 3 | 3 | 2 |
| β-84 | 75 | 83 | 78 | 83 |
| β-155 | 13 | 14 | 19 | 15 |

The energetic relaxation comprises radiative and non-radiative relaxation. Initial excitation was localized on α-84, β-84 and β-155, respectively. The stationary solution of excitation distribution from the rate equation is given for comparison.

fast energy transfer component from α-84 to β-84 either by fast Förster type transfer or by excitonic coupling.

### 3.6. Monte Carlo simulations of energy transfer in single PEC monomers

In earlier experiments with single PEC molecules, we observed heterogeneities in the energy transfer between different individual PEC molecules [8]. Monte Carlo simulations based on the Förster calculations presented here allow us to explain this experimental finding. From the simulations, we obtain the fraction of excitation energy which leaves PEC via relaxation of one of the chromophores. Relaxation can either occur radiatively by fluorescence emission or non-radiatively. In the single molecule experiments, we determine the fraction of β-subunit fluorescence originating from β-155 [8]. This fraction is defined as $\gamma=(I_{\beta\text{-}155})/(I_{\beta\text{-}84}+I_{\beta\text{-}155})$.

Here, $I_{xx}$ is the integral steady state fluorescence intensity originating from β-84 and β-155, respectively. In the experiment described in Ref. [8], $I_{xx}$ was not directly accessible. Therefore, $\gamma$ was extracted from single molecule measurements, in which the orientation and the fluorescence emission intensity of individual monomeric PEC molecules were determined. In experiments with 101 different molecules, we observed a broad distribution of $\gamma$. Suitable spectral filters were employed to suppress any emission from the α-84 chromophore in these experiments. In order to compare $\gamma$ with the energy distribution fractions gained from the Monte Carlo simulations, the latter have to be normalized to account for the neglect of α-84 emission in the single molecule experiment. It has been outlined above that the fluorescence quantum yields $\phi$ of the two PCB are assumed to be the same. For this reason, the normalized distribution fractions correspond directly to the fluorescence emission intensities. Förster energy transfer relies on several factors which could be responsible for changes in the energy transfer factor $\gamma$ and thus for the observed heterogeneities: Fluorescence lifetime changes of one chromophore can be excluded as they would only lead to different energy distribution and relaxation times, but not influence the rate ratios. Changes in the orientational parameter $\kappa$, the refractive index, and the interchromophoric distances influence the forward and backward rates equally. This will not lead to any differences in the distribution of energy in the Förster picture. However, while the rate ratios will not change, their absolute values can change significant-

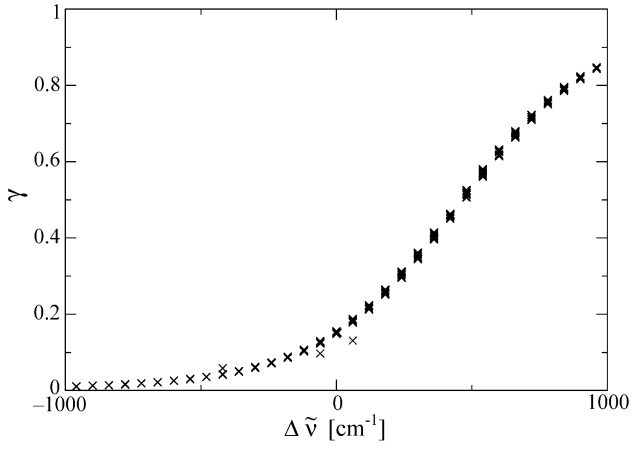


Fig. 3. The influence of relative spectral shifts $\Delta\tilde{\nu}$ between the β-84 and the β-155 PCB chromophores, on the energy transfer values $\gamma$ as determined from the Monte Carlo simulations. Spectral shifts of $\pm 1000$ cm$^{-1}$ were considered for each chromophore. Multiple values $\gamma$ appear due to the limited sampling depth of the simulation.

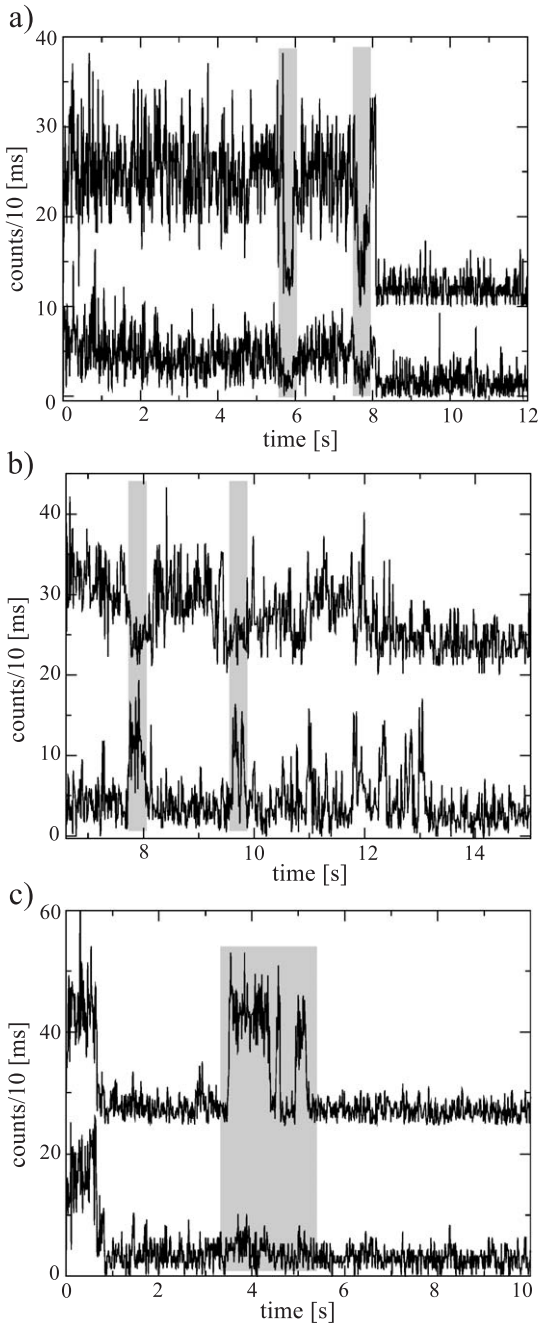


Fig. 4. Simultaneously detected emission intensities of two perpendicular polarization components of individual β-subunits. Three different behaviors are observed: (a) correlated emission, (b) anti-correlated emission, (c) non-correlated emission.

ly. Due to the comparable rates of energy transfer and (radiative and non-radiative) relaxation, the system might not be equilibrated before emission occurs. We therefore modeled a change of $\pm 20°$ in the angles defining the orientation of each chromophore, a change of 10% in the distance r between the chromophores, and a refractive index range from 1.33 (water) to 1.50 (glass). The changes in $\gamma$ which we obtained were $\Delta\gamma = 0.16$ (corresponding to $\gamma = 0.09 \pm 0.08$) for the different orientations, $\Delta\gamma = 0.02$ for the variations in $r$, and $\Delta\gamma = 0.004$ for the changes in the refractive index. We thus conclude that none of these factors is responsible for the observed heterogeneities in $\gamma$.

The other two remaining parameters are the fluorescence quantum yields of the chromophores and the spectral overlap integrals between them. Both of these can cause energy transfer heterogeneities. Fig. 3 shows the influence of changing the relative spectral position of the β-84 and the β-155 chromophore towards each other while keeping the Stokes shifts constant. It is clearly seen that already minor spectral shifts lead to major changes in $\gamma$. Fluctuations in the absorption and emission spectra of single molecules are well known [25–27]. At room temperature spectral jumps of more than 1000 $cm^{-1}$ have been reported, a much larger range than that necessary for a 100% change in $\gamma$. In this connection, it is also noteworthy that the spectra of PCB can change, even in the absence of linkers, by several tens of nanometer depending on the apoprotein (or chromophore site) to which it binds [3]. It therefore seems likely that shifts in the spectra of individual chromophores play an important role for the occurrence of the observed heterogeneities. While in earlier single molecule experiments, we only observed static heterogeneities which persisted over many seconds, we recently also detected dynamic heterogeneities. If only the emission of an individual β-subunit is detected, the fluorescence intensity trajectory can exhibit three different behaviors. Fig. 4 shows that indeed all possible sorts of behavior, namely the correlated, the uncorrelated and the anti-correlated emission of the two β-subunit chromophores, can be observed on a comparatively short time scale. The example for uncorrelated emission as in Fig. 4c can be explained by changes in the fluorescence quantum yields of one of the chromophores, due to the opening of non-radiative decay channels. If merely the spectra of this chromophore shifted far enough so that no energy transfer from α-84 onto this chromophore would occur, one would expect an increase in the fluorescence emission from the other chromophore. This, however, is not observed. A decrease in the fluorescence quantum yield of one β-chromophore, on the other hand, could lead to the observed behavior, as under this condition, the chromophore would still absorb but not fluoresce any more. By contrast, anti-correlated emission as in Fig. 4b can be caused by spectral shifts of one chromophore which will lead to on/off quenching of the fluorescence emission of the other chromophore.

In summary, we can describe energy transfer in monomeric PEC in a self-consistent way, based on the chromophore assignment of Parbel et al. [14]. The remarkable kinetic differences as compared to monomeric PC, which has a very similar structure, are mainly due to the α-84 phycoviolobilin chromophore characteristic for this biliprotein. Consideration of both, its changed spectrum and the structural dynamics, is necessary to rationalize the experimental data obtained with bulk as well as with single molecule spectroscopy.

## Acknowledgements

A.Z. and P.Z. thank C. Bräuchle for continuous support. This work was funded by the Deutsche Forschungsgemeinschaft, SFB 533, TP A1 and B7.

## References

[1] H. Scheer, The pigments, in: B. Green, W. Parson (Eds.), Light-Harvesting Antennas in Photosynthesis, Kluwer, Dordrecht, 2003, pp. 29–81.
[2] S. Schneider, W. Jäger, C.J. Prenzel, G. Brehm, P.S.M. Sai, H. Scheer, F. Lottspeich, Photophysics of phycoerythrocyanins from the cyanobacterium *Westiellopsis prolifica* studied by time-resolved fluorescence and coherent anti-Stokes–Raman scattering spectroscopy, J. Photochem. Photobiol., B Biol. 26 (1994) 75–85.
[3] A.R. Holzwarth, Structure–function relationships and energy-transfer in phycobiliprotein antennae, Physiol. Plant. 83 (1991) 518–528.
[4] M. Hucke, G. Schweitzer, A.R. Holzwarth, W. Sidler, H. Zuber, Studies on chromophore coupling in isolated phycobiliproteins. 4. Femtosecond transient absorption study of ultrafast excited-state dynamics in trimeric phycoerythrocyanin complexes, Photochem. Photobiol. 57 (1993) 76–80.
[5] P.S.M. Sai, S. Siebzehnrübl, S. Mahajan, H. Scheer, Fluorescence and circular dichroism studies on the phycoerythrocyanins from the cyanobacterium *Westiellopsis prolifica*, Photochem. Photobiol. 57 (1993) 71–75.
[6] M. Dürring, R. Huber, W. Bode, R. Rümbeli, H. Zuber, Refined 3-dimensional structure of phycoerythrocyanin from the cyanobacterium *Mastigocladus laminosus* at 2.7 Å, J. Mol. Biol. 211 (1990) 633–644.
[7] T. Förster, Delocalized excitation and excitation transfer, in: O. Sinanoglu (Ed.), Modern Quantum Chemistry: Part III. Action of Light and Organic Crystals, Academic Press, New York, 1965, pp. 93–117.
[8] P. Zehetmayer, T. Hellerer, A. Parbel, H. Scheer, A. Zumbusch, Spectroscopy of single phycoerythrocyanin monomers: dark state identification and observation of energy transfer heterogeneities, Biophys. J. 83 (2002) 407–415.
[9] R.W. Castenholz, Laboratory culture of thermophylic cyanophytes, Schweiz. Z. Hydrol. 35 (1970) 538–551.
[10] P. Füglistaller, H. Widmer, W. Sidler, G. Frank, H. Zuber, Isolation and characterization of phycoerythrocyanin and chromatic adaptation of the thermophilic cyanobacterium *Mastigocladus laminosus*, Arch. Microbiol. 129 (1981) 268–274.
[11] A. Parbel, Charakterisierung von Phycobiliprotein-Linkerkomplexen aus dem Phycobilisom von *Mastigocladus laminosus*, Dissertation, Ludwig-Maximillians Universität, München, 1997.
[12] W. Reuter, Spektrale, strukturelle und biochemische Charakterisierung des Phycobilisomenzentrums und einiger Konstituenten der Phycobilisomenperipherie von *Mastigocladus laminosus* unter Berücksichtigung der Funktion, Dissertation, Philipps-Universität, Marburg, 1989.

[13] G. Wiegand, A. Parbel, M.H.J. Seifert, T.A. Holak, W. Reuter, Purification, crystallization, NMR spectroscopy and biochemical analyses of α-phycoerythrocyanin peptides, Eur. J. Biochem. 269 (2002) 5046–5055.
[14] A. Parbel, K.H. Zhao, J. Breton, H. Scheer, Chromophore assignment in phycoerythrocyanin from *Mastigocladus laminosus*, Photosynth. Res. 54 (1997) 25–34.
[15] J. Lakowicz, Principles of Fluorescence Spectroscopy, Kluwer Academic/Plenum Publishers, New York, 1999.
[16] R.S. Moog, A. Kuki, M.D. Fayer, S.G. Boxer, Excitation transport and trapping in a synthetic chlorophyllide substituted hemoglobin-orientation of the chlorophyll-S1 transition dipole, Biochemistry 23 (1984) 1564–1571.
[17] M. Matsumoto, T. Nishimura, Mersenne twister: a 623-dimensionally equidistributed uniform pseudorandomnumber generator, ACM Trans. Model. Comput. Simul. 8 (1998) 3–30.
[18] M.P. Debreczeny, K. Sauer, J.H. Zhou, D.A. Bryant, Monomeric C-phycocyanin at room-temperature and 77 K-resolution of the absorption and fluorescence-spectra of the individual chromophores and the energy-transfer rate constants, J. Phys. Chem. 97 (1993) 9852–9862.
[19] H. Förstendorf, A. Parbel, H. Scheer, F. Siebert, Z,E isomerization of the α-84 phycoviolobilin chromophore of phycoerythrocyanin from *Mastigocladus laminosus* investigated by Fourier-transform infrared difference spectroscopy, FEBS Lett. 402 (1997) 173–176.
[20] P.S.M. Sai, S. Siebzehnrübl, S. Mahajan, H. Scheer, Phycoerythrocyanins from *Westiellopsis prolifica* and *Nostoc rivulare*—characterization of the phycoviolobilin chromophore in both states, Photochem. Photobiol. 55 (1992) 119–124.
[21] D.F. Eaton, Reference materials for fluorescence measurement, Pure Appl. Chem. 60 (1988) 1107–1114.
[22] M.P. Debreczeny, K. Sauer, J.H. Zhou, D.A. Bryant, Comparison of calculated and experimentally resolved rate constants for excitation-energy transfer in C-phycocyanin. 1. Monomers, J. Phys. Chem. 99 (1995) 8412–8419.
[23] J.S. Kang, G. Piszczek, J.R. Lakowicz, Enhanced emission induced by FRET from a long-lifetime, low quantum yield donor to a long-wavelength, high quantum yield acceptor, J. Fluoresc. 12 (2002) 97–103.
[24] T. Schirmer, W. Bode, R. Huber, Refined 3-dimensional structures of 2 cyanobacterial C-phycocyanins at 2.1 and 2.5 Å resolution—a common principle of phycobilin–protein interaction, J. Mol. Biol. 196 (1987) 677–695.
[25] Y. Durand, A. Bloess, A.M. van Oijen, J. Köhler, E.J.J. Groenen, J. Schmidt, An optical study of single pentacene molecules in *n*-tetradecane, Chem. Phys. Lett. 317 (2000) 232–237.
[26] H.P. Lu, X.S. Xie, Single-molecule spectral fluctuations at room temperature, Nature 385 (1997) 143–146.
[27] C. Blum, F. Stracke, S. Becker, K. Müllen, A.J. Meixner, Discrimination and interpretation of spectral phenomena by room-temperature single-molecule spectroscopy, J. Phys. Chem., A 105 (2001) 6983–6990.